Supplement of Nat. Hazards Earth Syst. Sci., 17, 409–421, 2017
http://www.nat-hazards-earth-syst-sci.net/17/409/2017/
doi:10.5194/nhess-17-409-2017-supplement

Natural Hazards and Earth System Sciences
Open Access
EGU

Supplement of

Assessment of reliability of extreme wave height prediction models

Satish Samayam et al.

Correspondence to: Sannasiraj Sannasi Annamalaisamy (sasraj@iitm.ac.in)

This supplementary material comprises of maps showing the study locations and all the plots of GEV, GPD and P-app model analysis for all locations considered in this study.

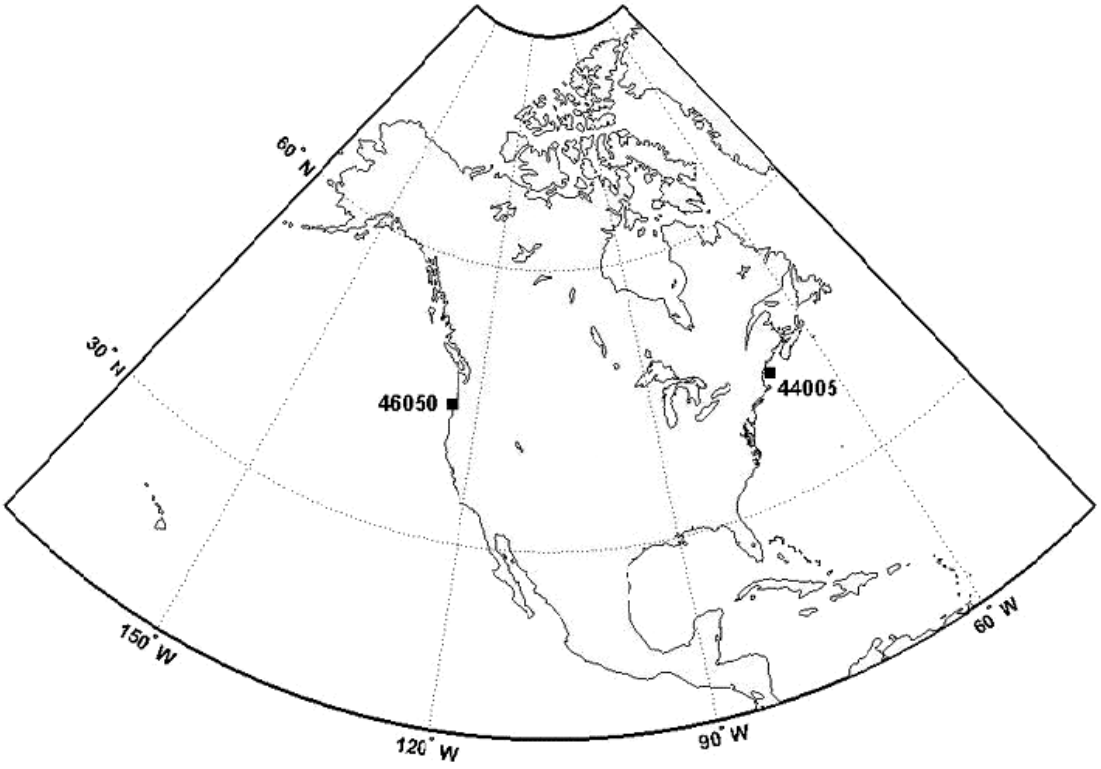

Fig. 1: Selected NOAA-National Data Buoy Centre Station locations

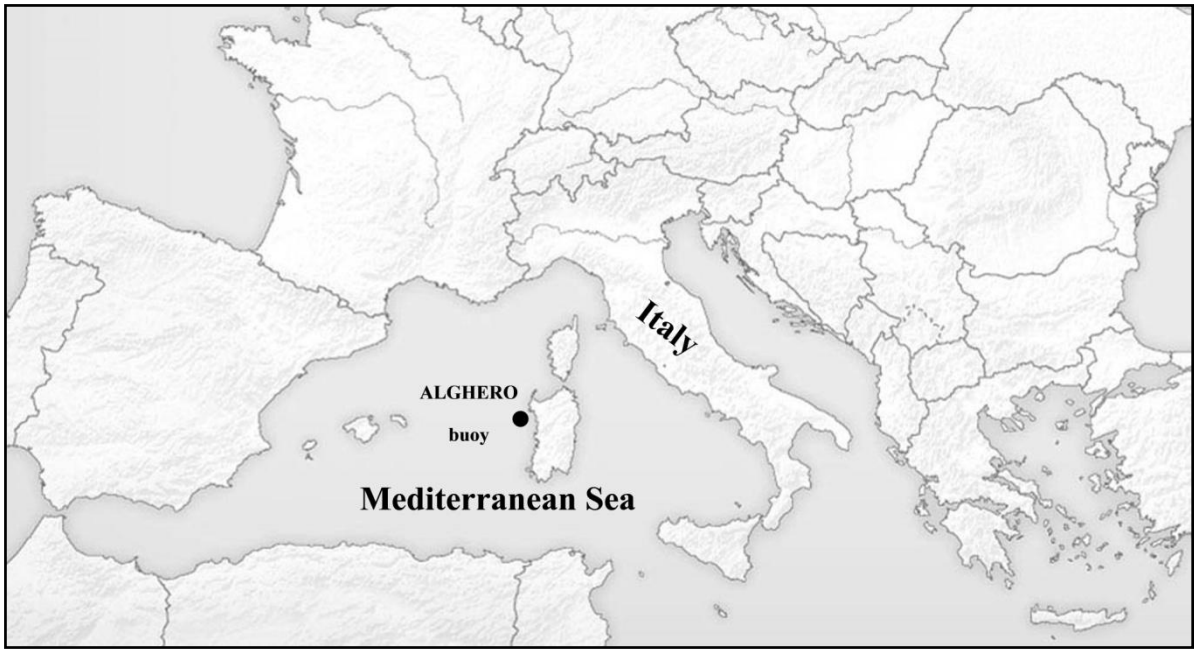

Fig. 2: Location of Alghero buoy in Mediterranean Sea

GEV DISTRIBUTION MODEL ANALYSIS

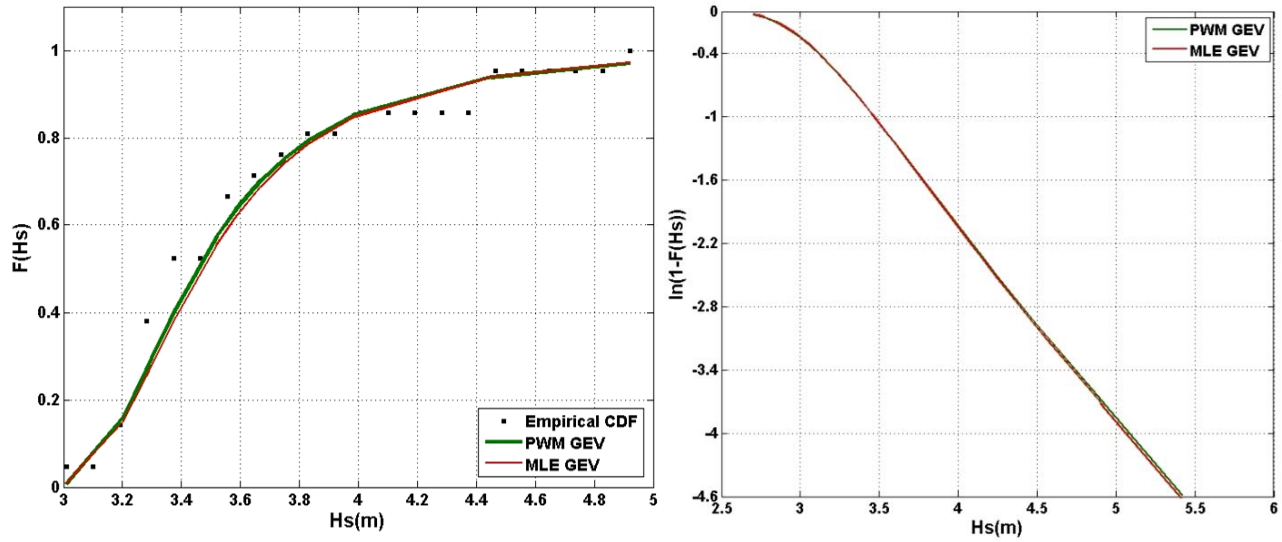

Fig. 3(a): Comparison of GEV model CDF to the empirical CDF for ERA IN-1

(b): Variation of tail GEV model CDF in logarithmic coordinates for ERA IN-1

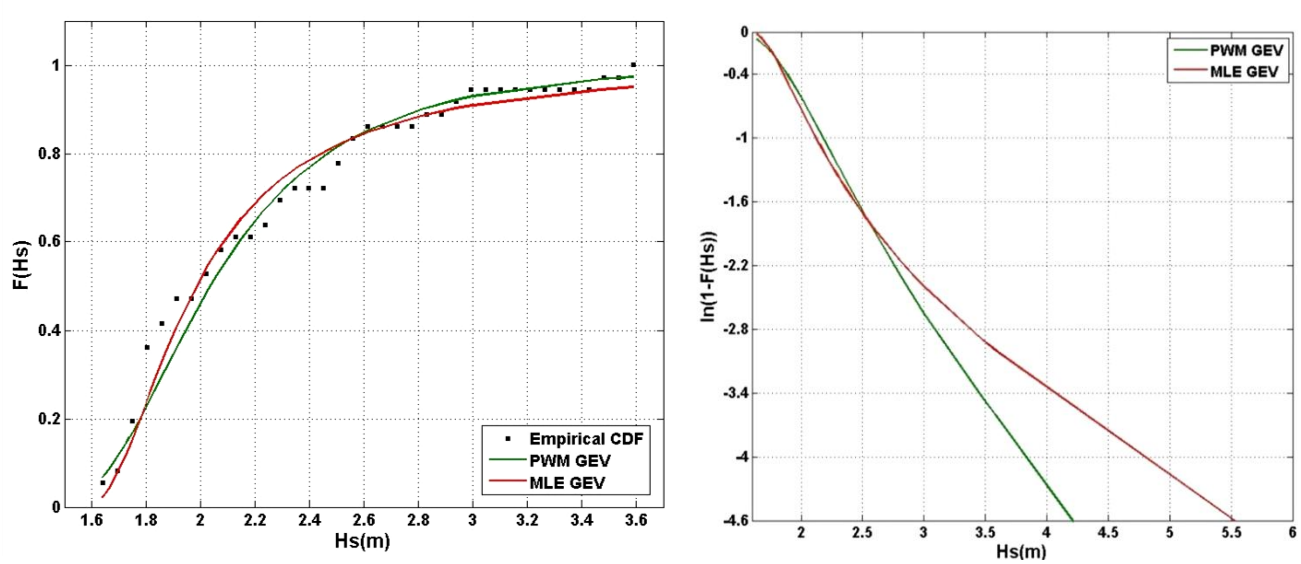

Fig. 4(a) : Comparison of GEV model CDF to the empirical CDF for ERA IN-2

(b) : Variation of tail GEV model CDF in logarithmic coordinates for ERA IN-2

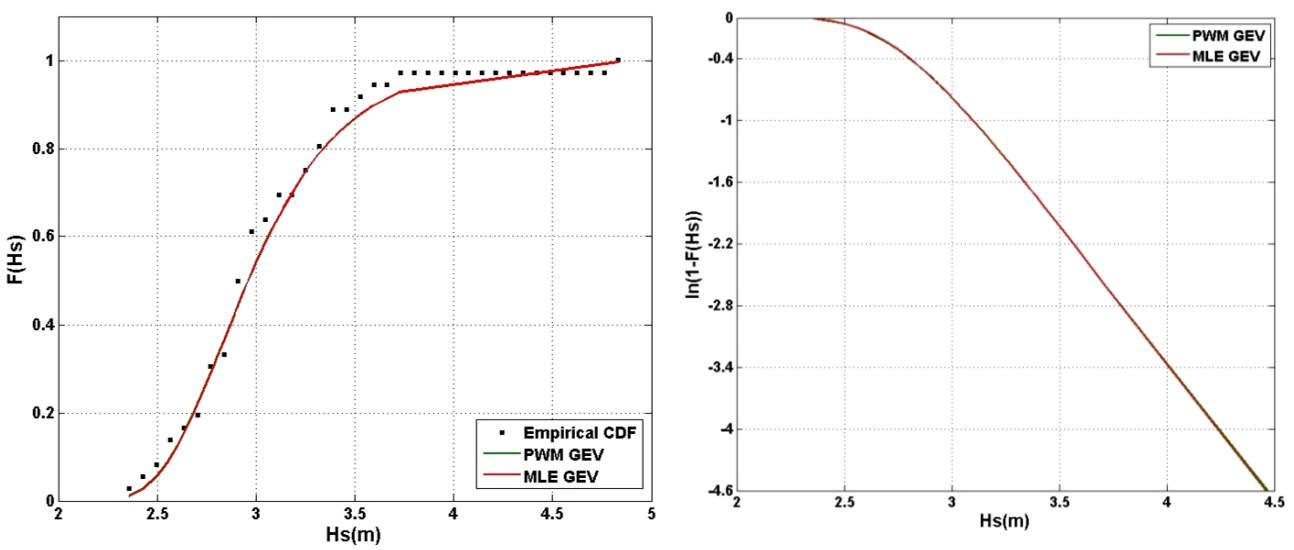

Fig. 5 (a) : Comparison of GEV model CDF to the empirical CDF for ERA IN-3

(b): Variation of tail GEV model CDF in logarithmic coordinates for ERA IN-3

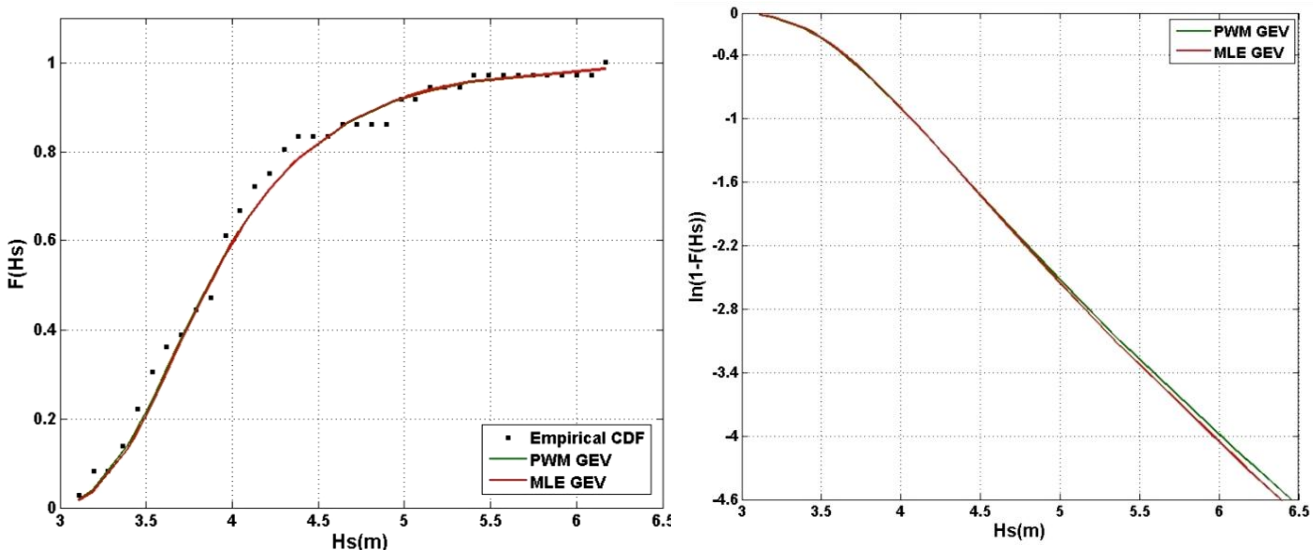

Fig. 6(a): Comparison of GEV model CDF to the empirical CDF for ERA IN-4

(b): Variation of tail GEV model CDF in logarithmic coordinates for ERA IN-4

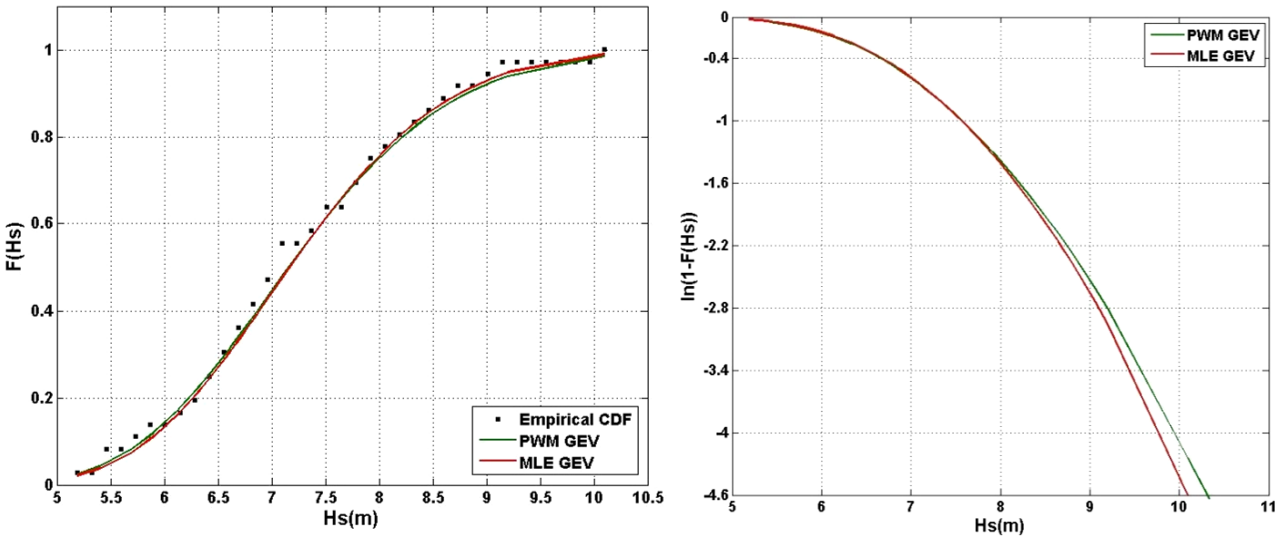

Fig. 7(a): Comparison of GEV model CDF to the empirical CDF for NOAA 44005

(b): Variation of tail GEV model CDF in logarithmic coordinates for NOAA 44005

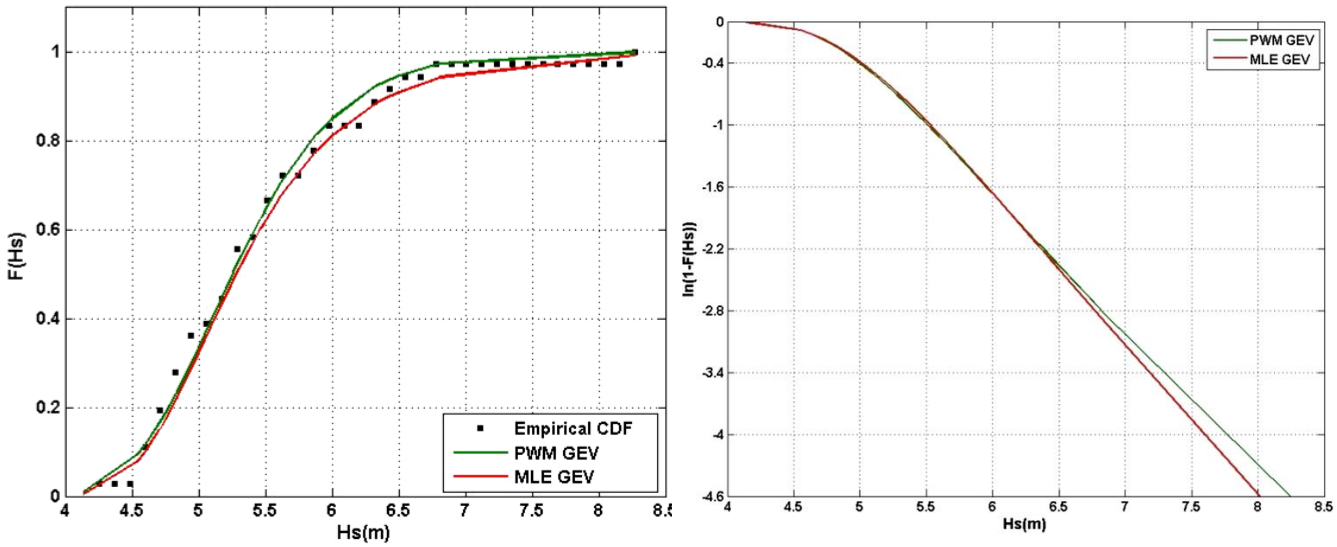

Fig. 8(a): Comparison of GEV model CDF to the empirical CDF for ERA 44005

(b): Variation of tail GEV model CDF in logarithmic coordinates for ERA 44005

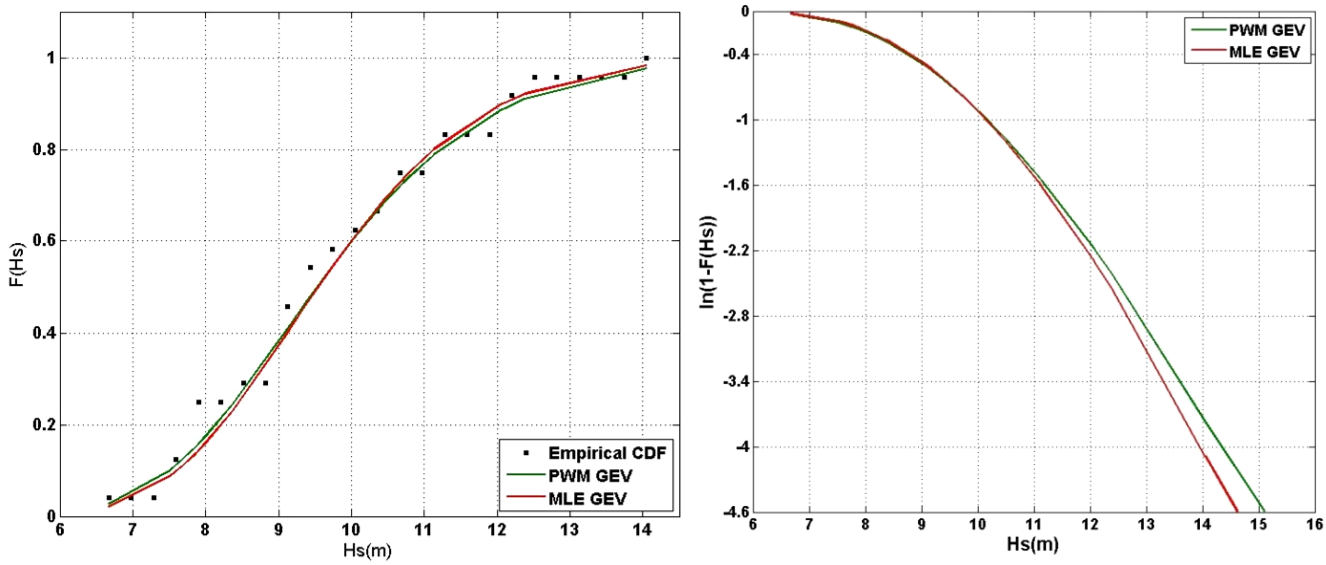

Fig. 9(a): Comparison of GEV model CDF to the empirical CDF for NOAA 46050

(b): Variation of tail GEV model CDF in logarithmic coordinates for NOAA 46050

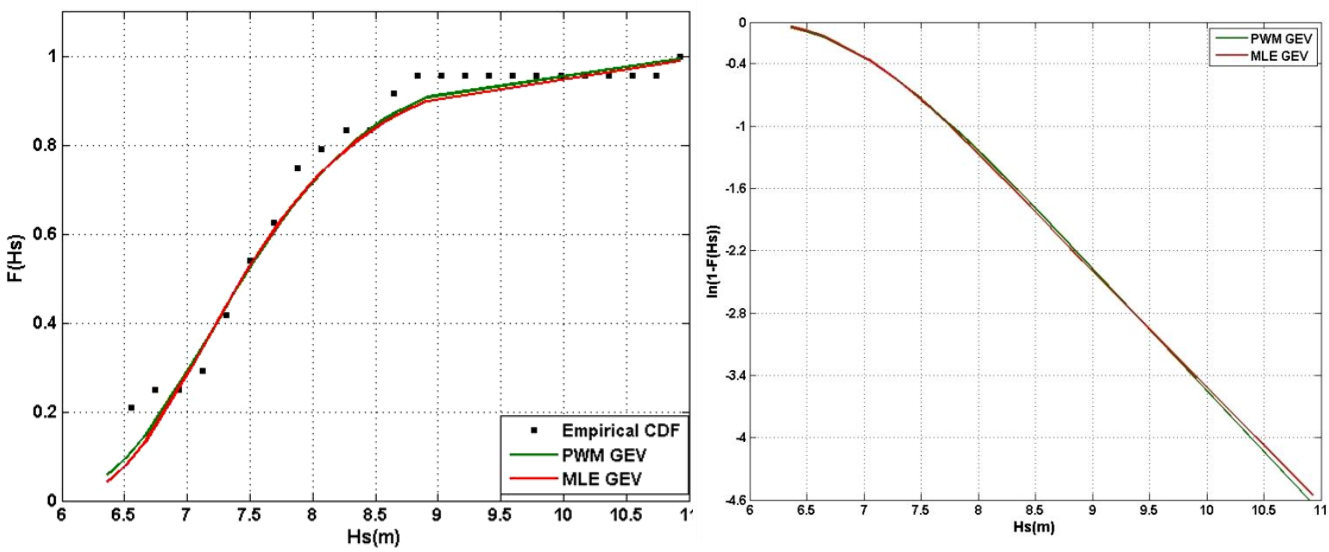

Fig. 10(a): Comparison of GEV model CDF to the empirical CDF for ERA 46050

(b): Variation of tail GEV model CDF in logarithmic coordinates for ERA 46050

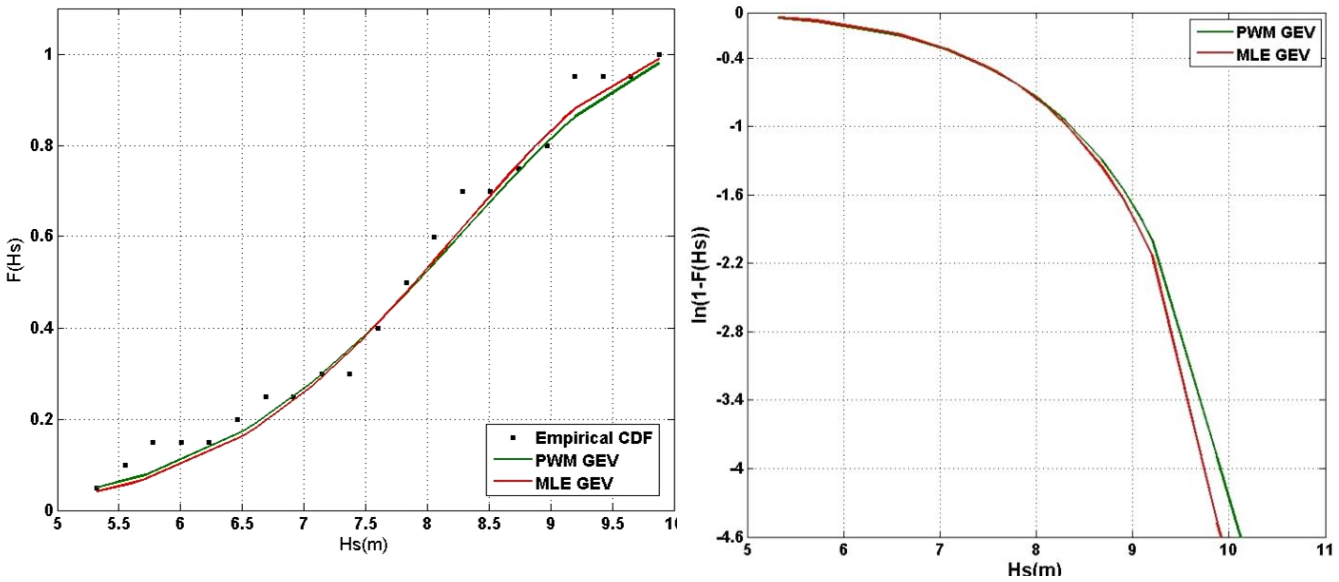

Fig. 11(a): Comparison of GEV model CDF to the empirical CDF for RON Alghero

(b) : Variation of tail GEV model CDF in logarithmic coordinates for RON Alghero

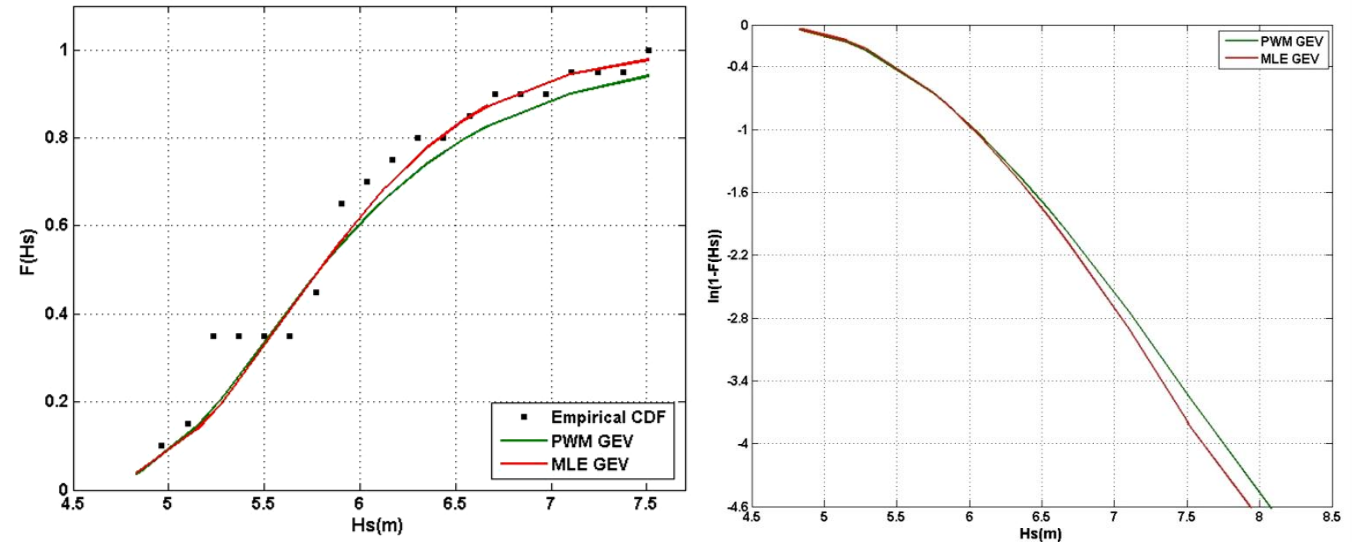

Fig. 12(a): Comparison of GEV model CDF to the empirical CDF for ERA Alghero

(b): Variation of tail GEV model CDF in logarithmic coordinates for ERA Alghero

GENERALISED PARETO DISTRIBUTION ANALYSIS

···· 95% Confidence Interval —— Fitted PWM GPD model ᴰᴰᴰᴰ POT sampled data

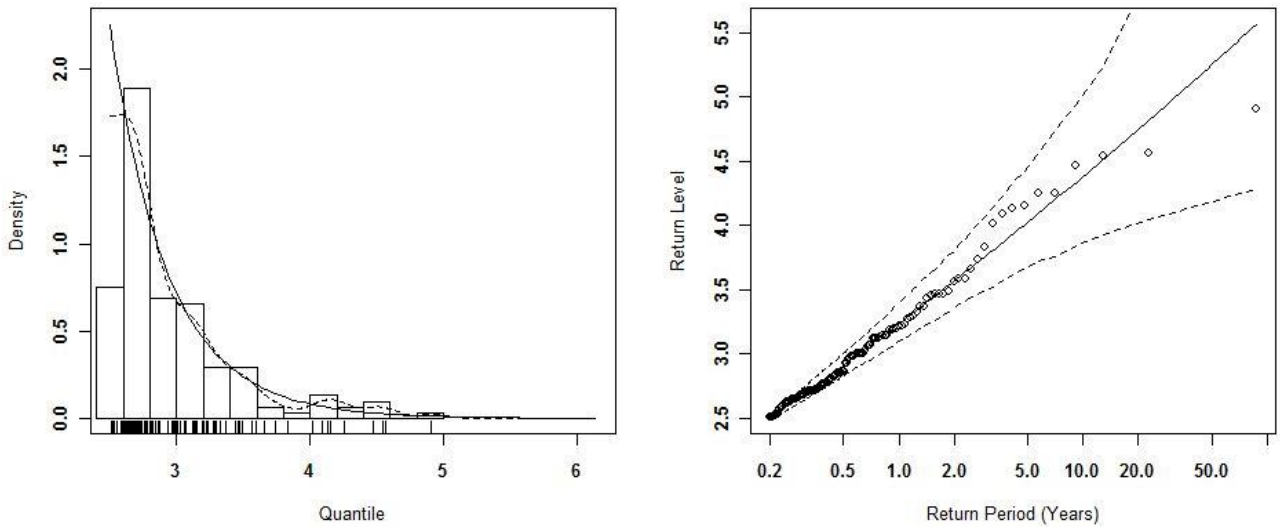

(a) **(b)**

Fig. 13 :(a) Density plot of GPD model for ERA IN-1 POT data from PWM method

(b) Return level plot of GPD model for ERA IN-1 POT data from PWM method

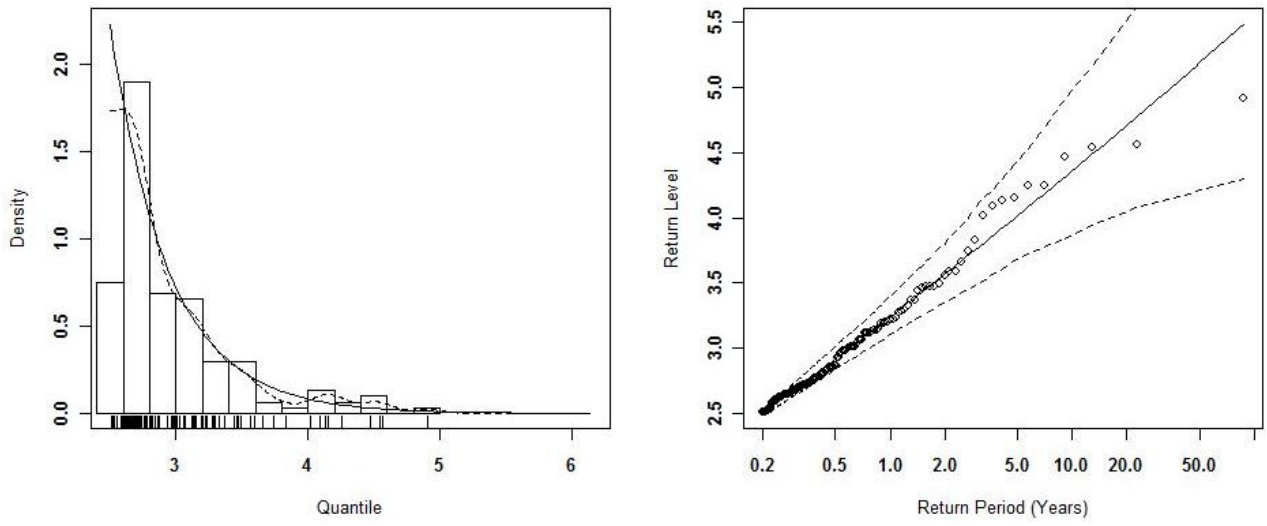

(a) **(b)**

Fig. 14 :(a) Density plot of GPD model for ERA IN-1 POT data from MLE method

(b) Return level plot of GPD model for ERA IN-1 POT data from MLE method

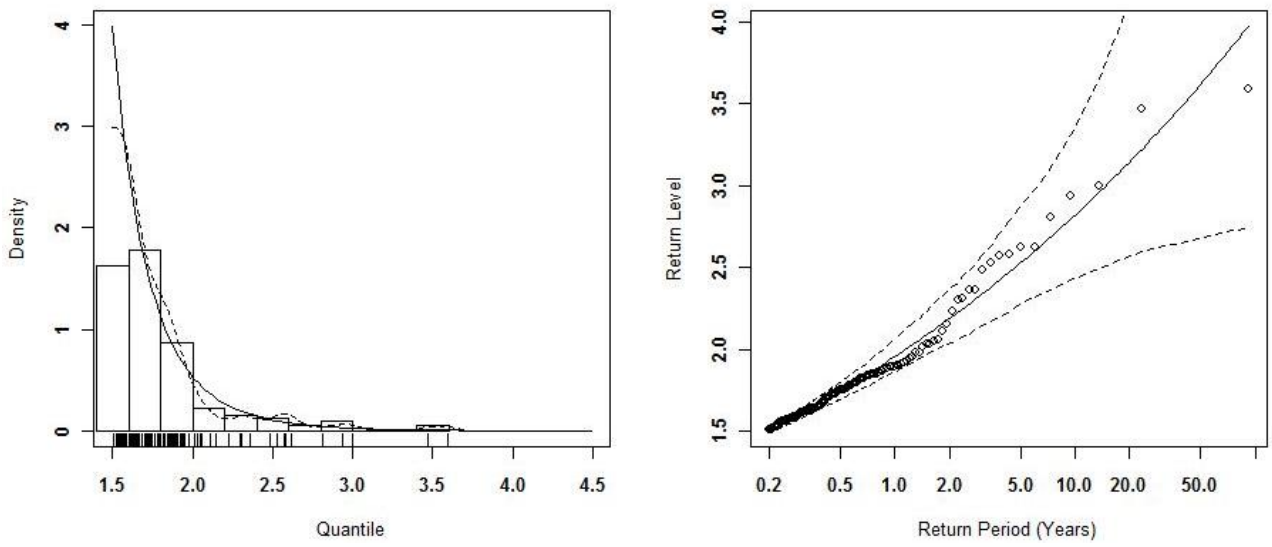

(a) **(b)**

Fig. 15 :(a) Density plot of GPD model for ERA IN-2 POT data from PWM method

(b) Return level plot of GPD model for ERA IN-2 POT data from PWM method

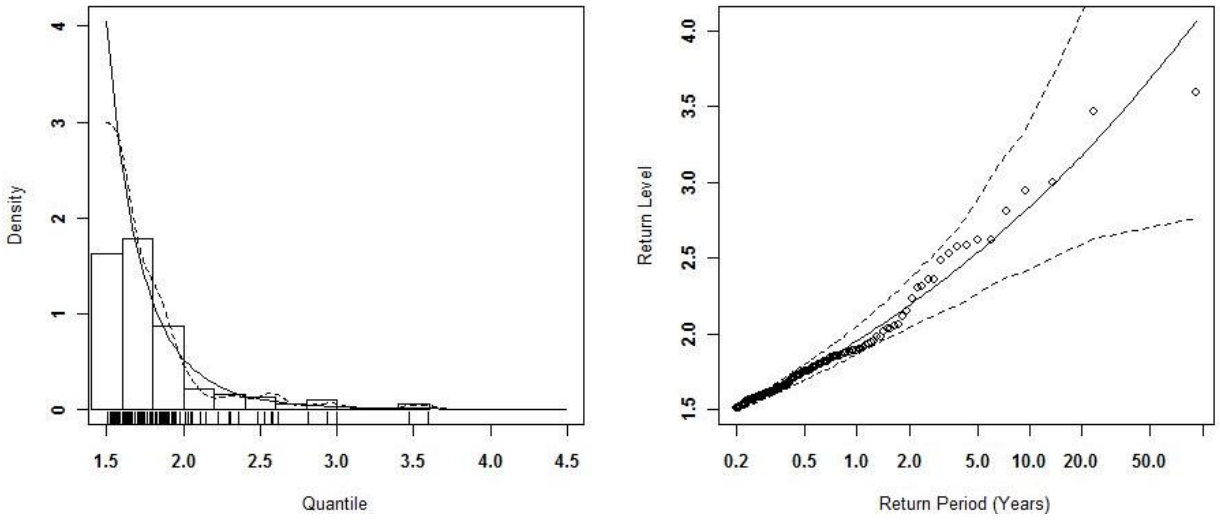

(a) **(b)**

Fig. 16 :(a) Density plot of GPD model for ERA IN-2 POT data from MLE method

(b) Return level plot of GPD model for ERA IN-2 POT data from MLE method

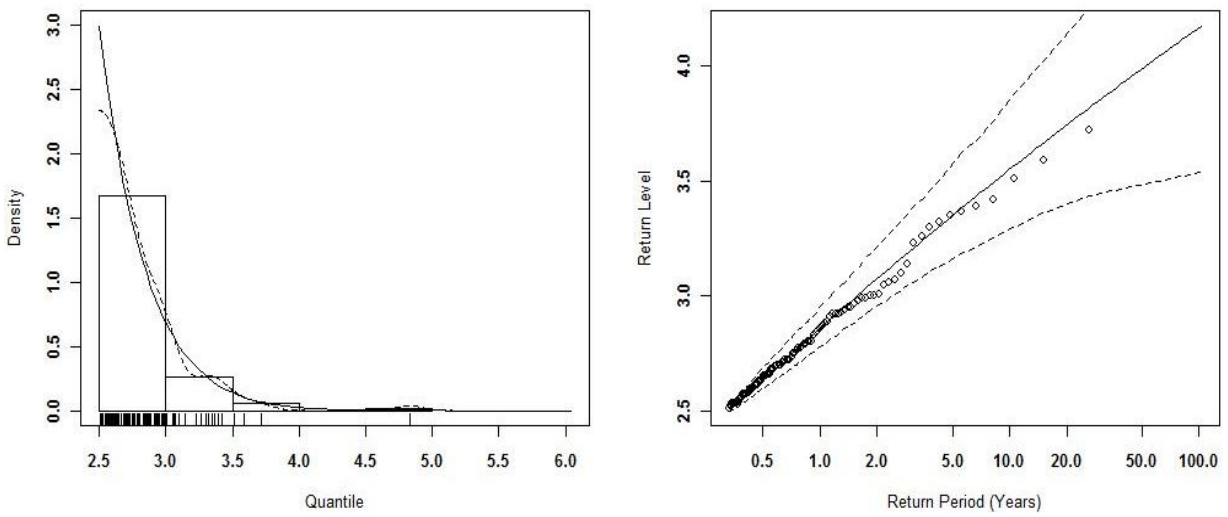

(a) **(b)**

Fig. 17 :(a) Density plot of GPD model for ERA IN-3 POT data from PWM method

(b) Return level plot of GPD model for ERA IN-3 POT data from PWM method

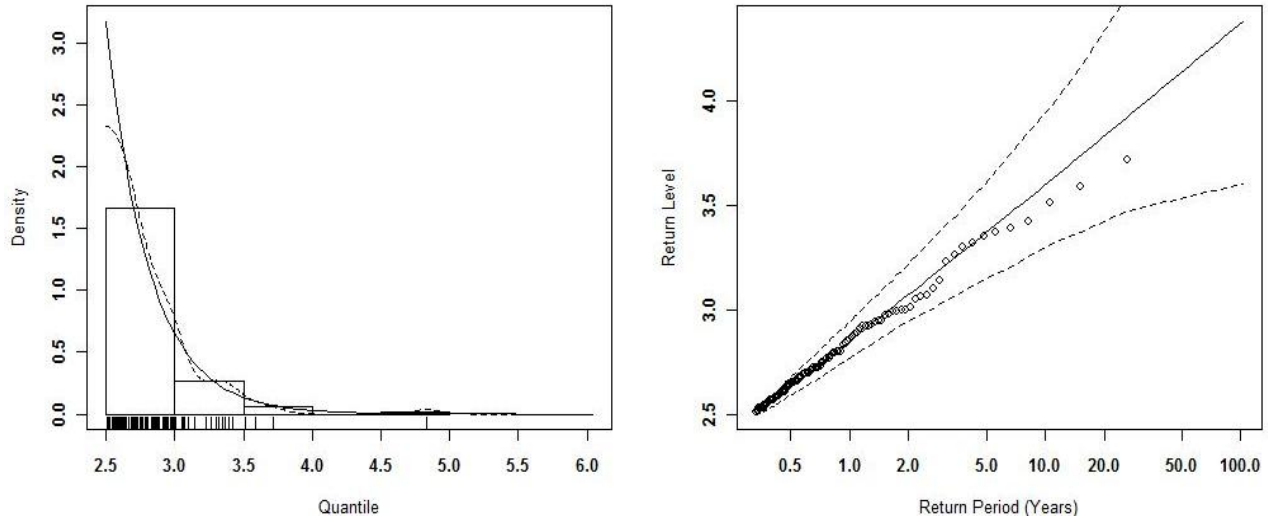

(a) **(b)**

Fig. 18 :(a) Density plot of GPD model for ERA IN-3 POT data from MLE method

(b) Return level plot of GPD model for ERA IN-3 POT data from MLE method

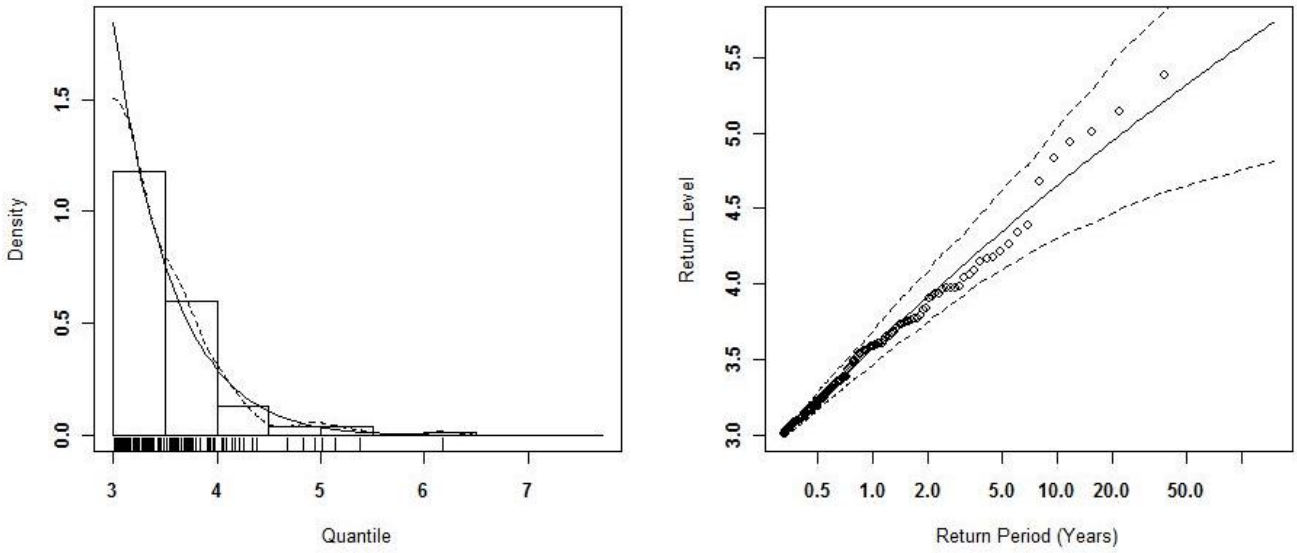

(a) **(b)**

Fig. 19 : (a) Density plot of GPD model for ERA IN-4 POT data from PWM method

(b) Return level plot of GPD model for ERA IN-4 POT data from PWM method

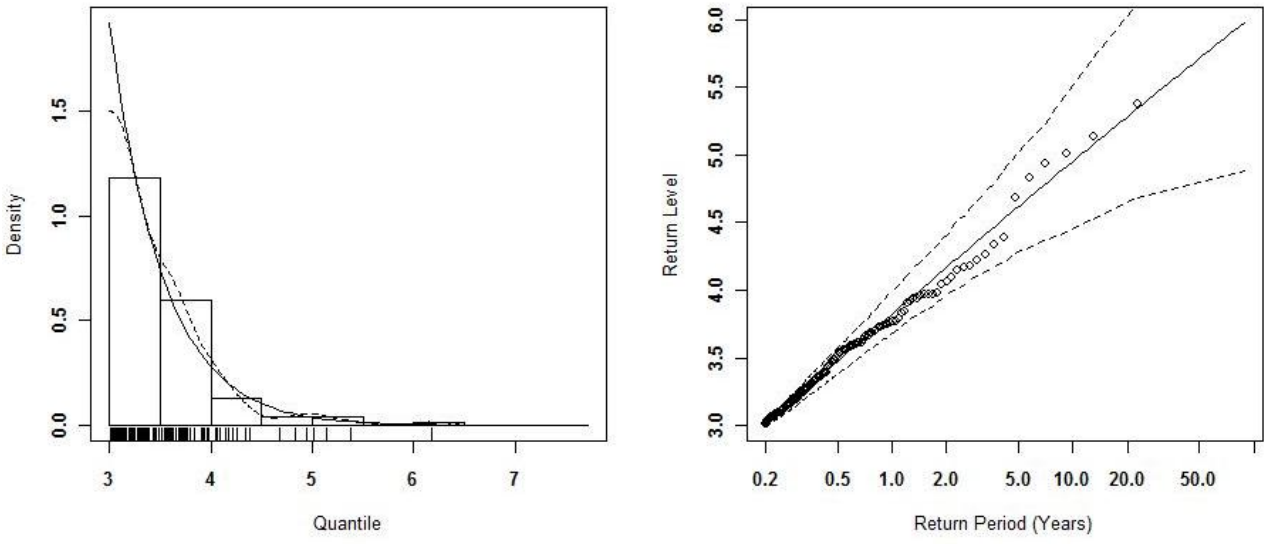

(a) **(b)**

Fig. 20 :(a) Density plot of GPD model for ERA IN-4 POT data from MLE method

(b) Return level plot of GPD model for ERA IN-4 POT data from MLE method

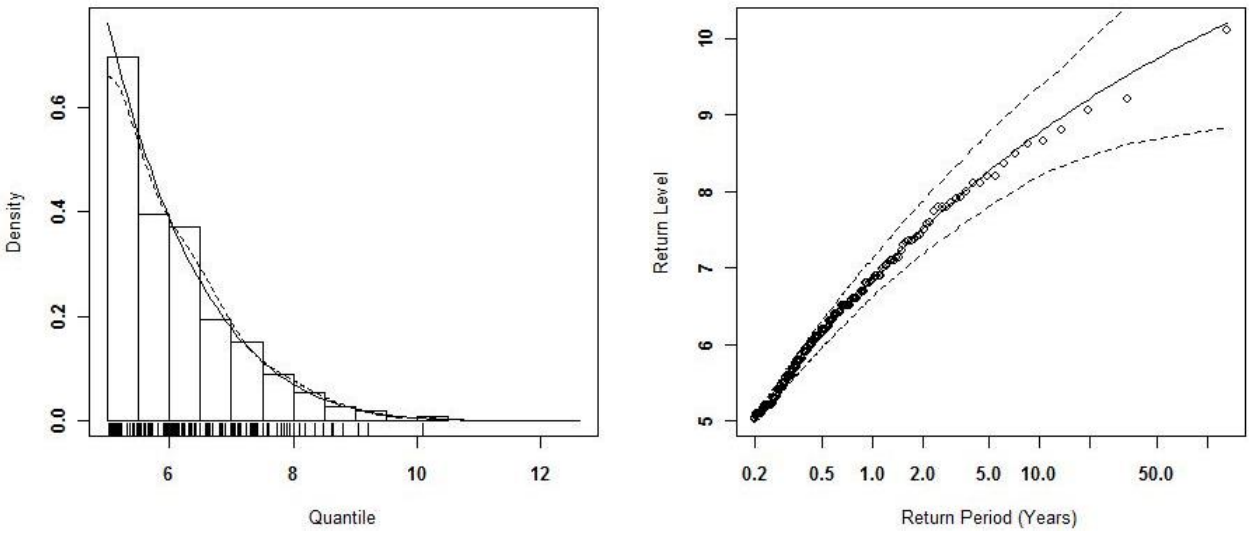

(a) **(b)**

Fig. 21 : (a) Density plot of GPD model for NOAA44005 POT data from PWM method

(b) Return level plot of GPD model for NOAA44005 POT data from PWM method

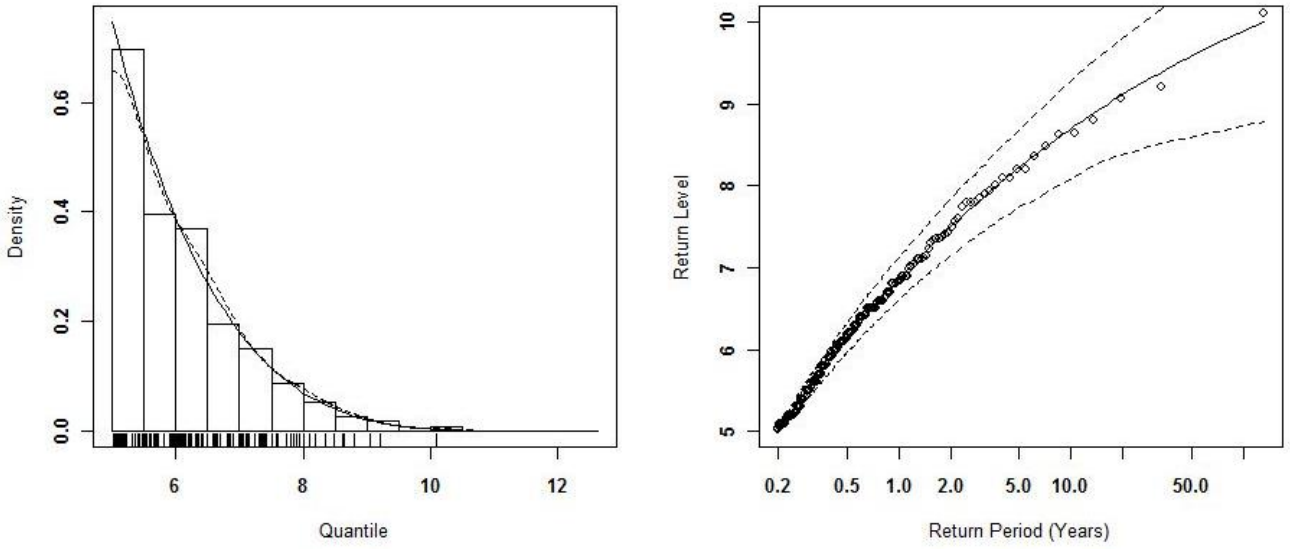

(a) **(b)**

Fig. 22 : (a) Density plot of GPD model for NOAA44005 POT data from MLE method

(b) Return level plot of GPD model for NOAA44005 POT data from MLE method

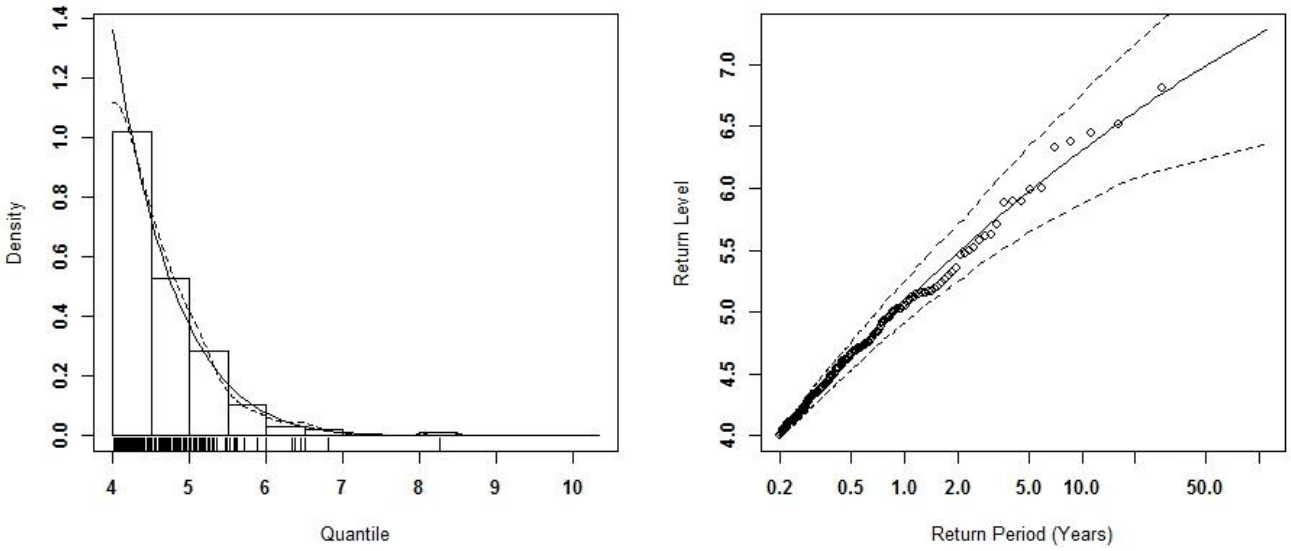

(a) **(b)**

Fig. 23 : (a) Density plot of GPD model for ERA 44005 POT data from PWM method

(b) Return level plot of GPD model for ERA 44005 POT data from PWM method

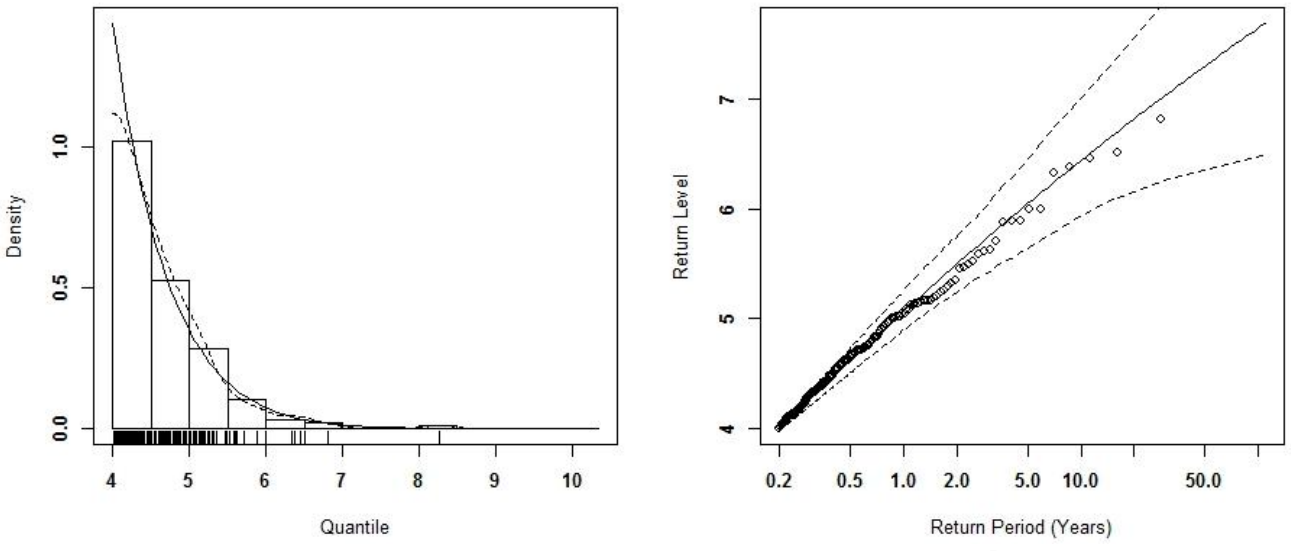

(a) **(b)**

Fig. 24 : (a) Density plot of GPD model for ERA 44005 POT data from MLE method

(b) Return level plot of GPD model for ERA 44005 POT data from MLE method

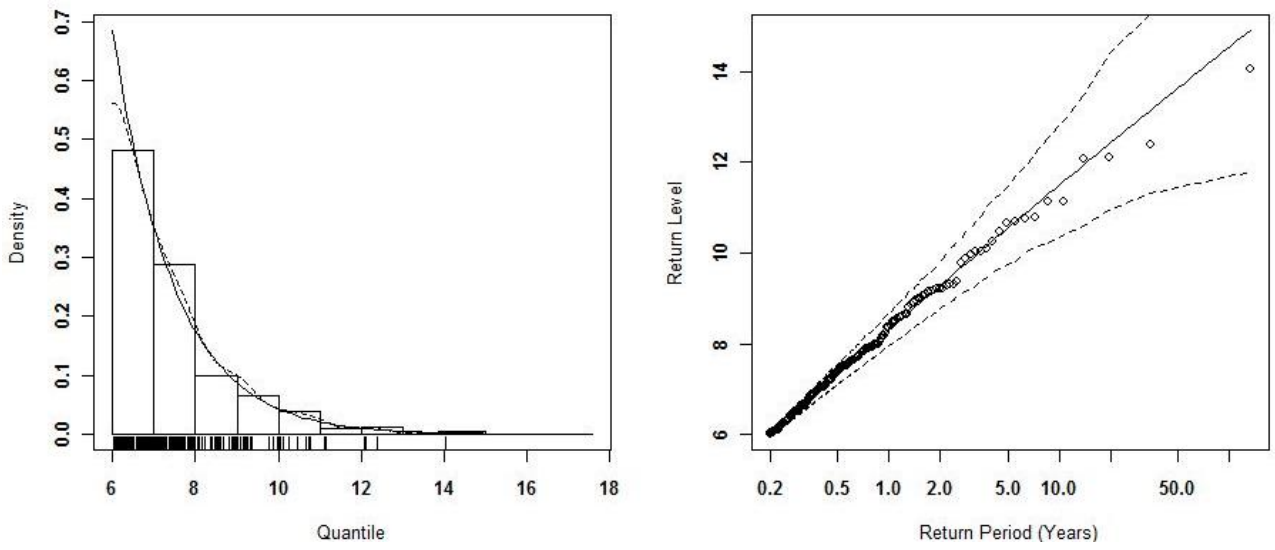

(a) **(b)**

Fig. 25 :(a) Density plot of GPD model for NOAA 46050 POT data from PWM method

(b) Return level plot of GPD model for NOAA 46050 POT data from PWM method

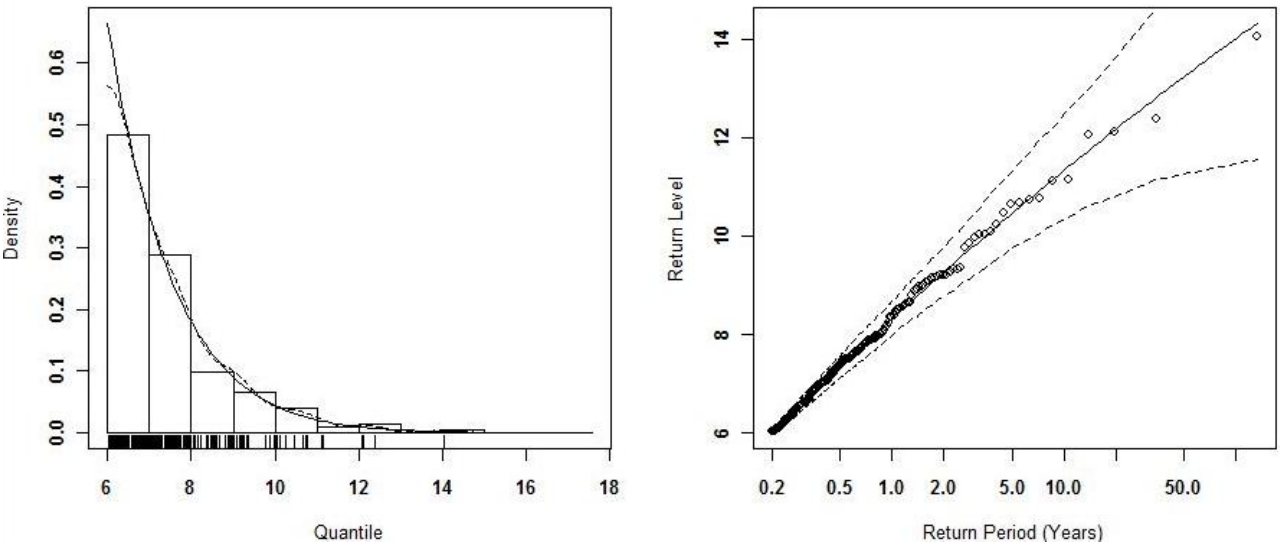

(a) **(b)**

Fig. 26 :(a) Density plot of GPD model for NOAA 46050 POT data from MLE method

(b) Return level plot of GPD model for NOAA 46050 POT data from MLE method

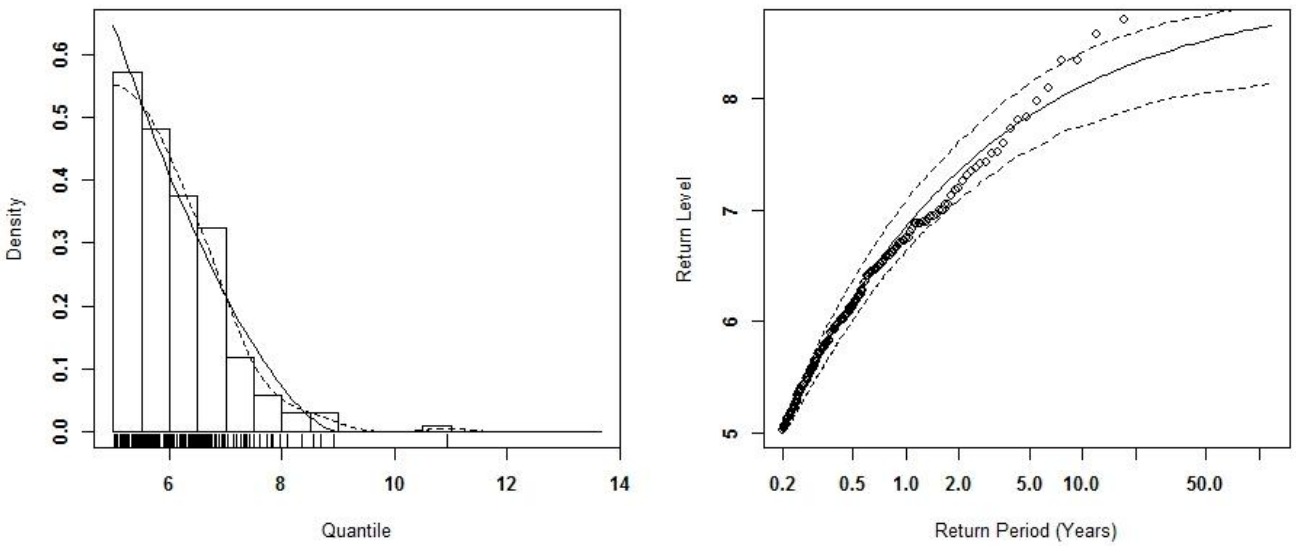

(a) **(b)**

Fig. 27 :(a) Density plot of GPD model for ERA 46050 POT data from PWM method

(b) Return level plot of GPD model for ERA 46050 POT data from PWM method

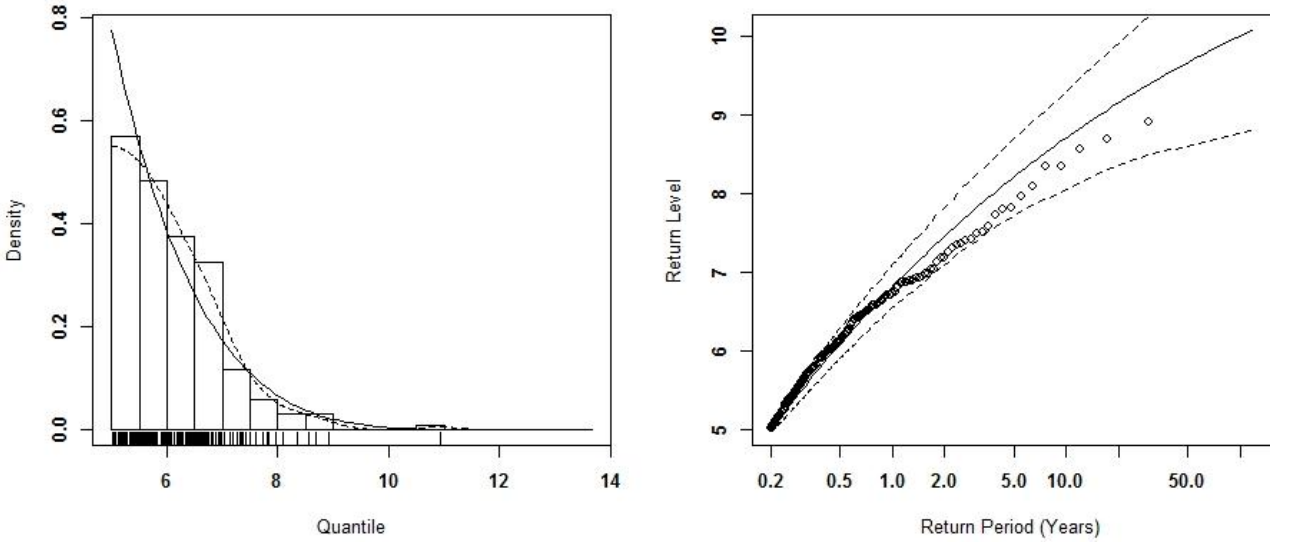

(a) **(b)**

Fig. 28 :(a) Density plot of GPD model for ERA 46050 POT data from MLE method

(b) Return level plot of GPD model for ERA 46050 POT data from MLE method

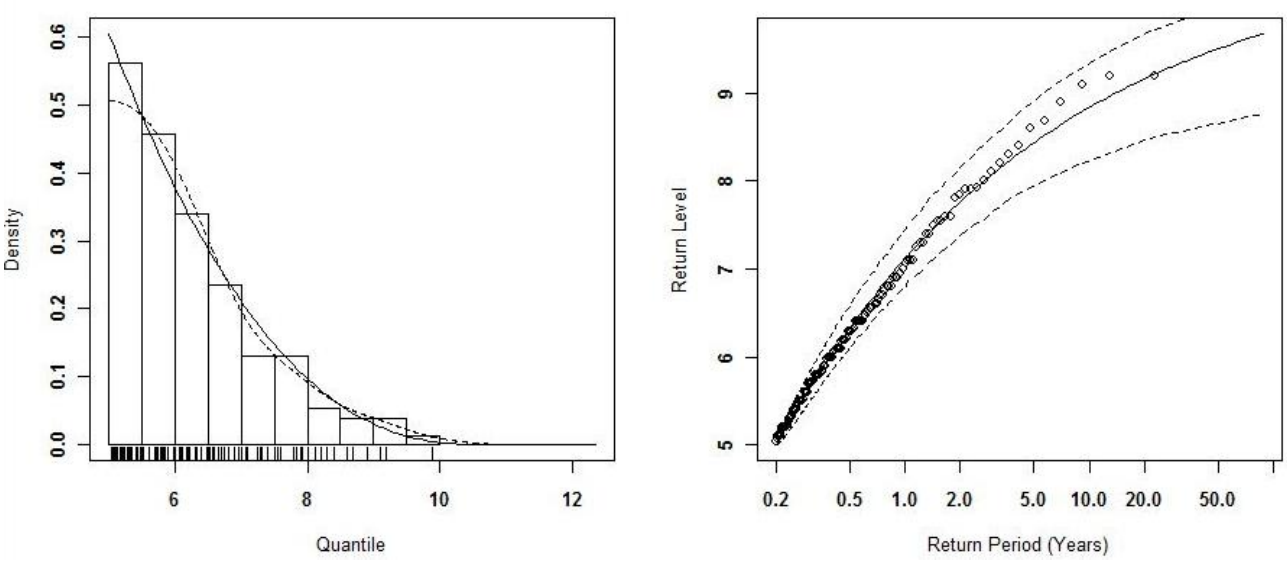

(a) **(b)**

Fig. 29 :(a) Density plot of GPD model for Alghero Buoy POT data from PWM method

(b) Return level plot of GPD model for Alghero Buoy POT data from PWM method

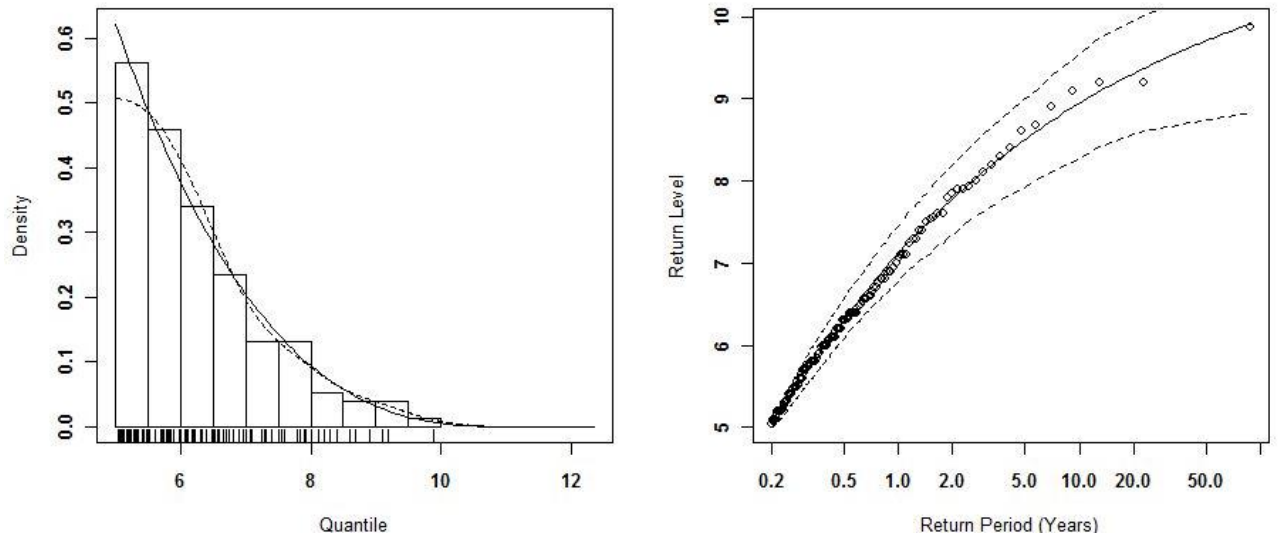

(a) **(b)**

Fig. 30 :(a) Density plot of GPD model for Alghero Buoy POT data from MLE method

(b) Return level plot of GPD model for Alghero Buoy POT data from MLE method

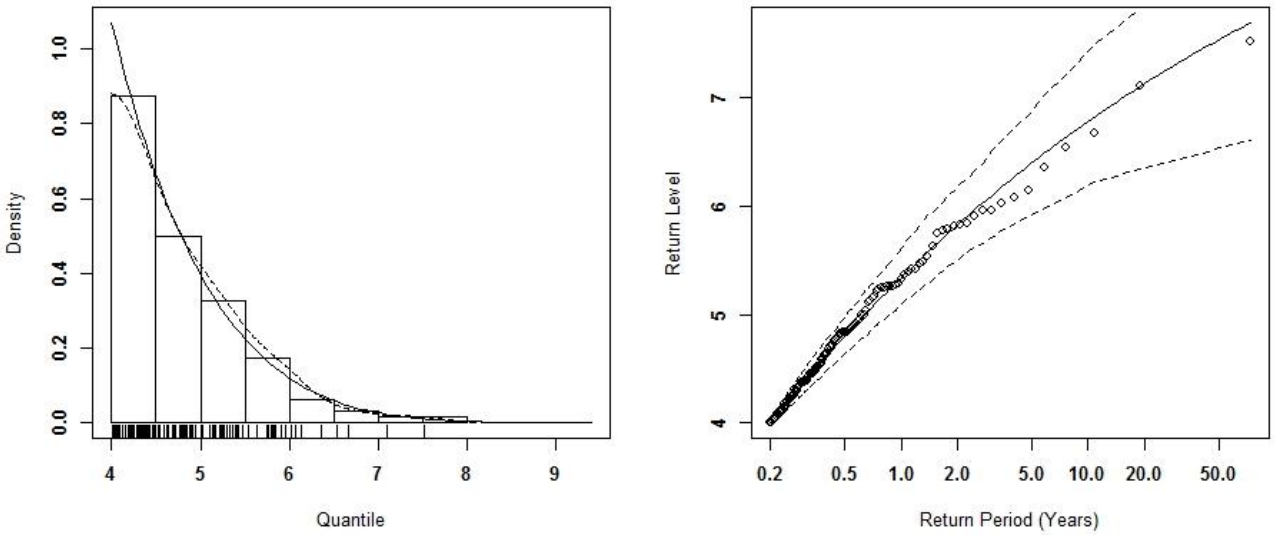

(a) **(b)**

Fig. 31 :(a) Density plot of GPD model for ERA Alghero POT data from PWM method

(b) Return level plot of GPD model for ERA Alghero POT data from PWM method

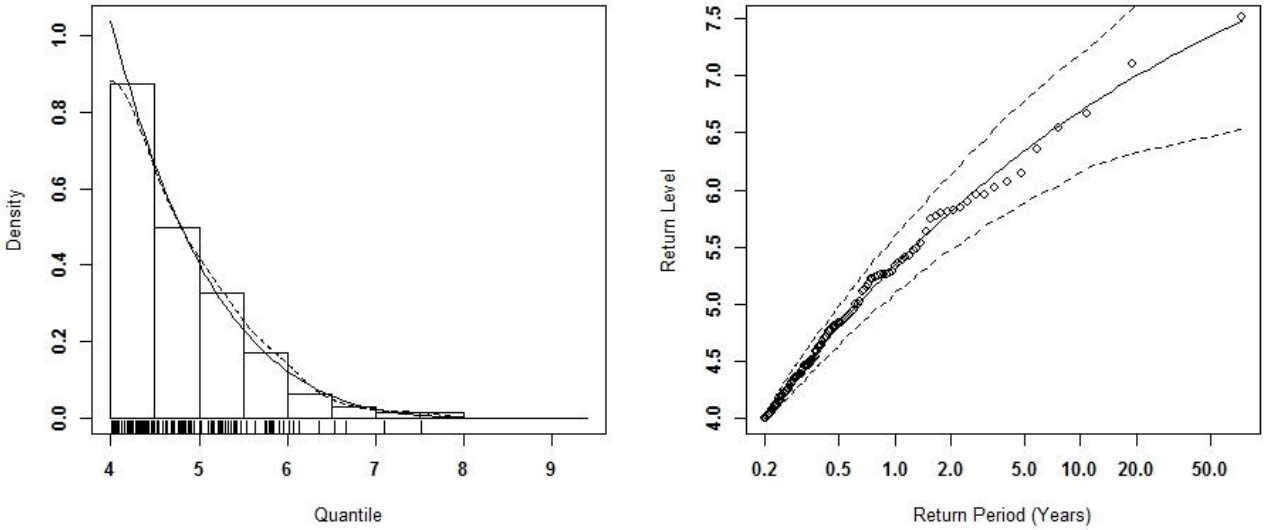

(a) **(b)**

Fig. 32 : (a) Density plot of GPD model for ERA Alghero POT data from MLE method

(b) Return level plot of GPD model for ERA Alghero POT data from MLE method

POLYNOMIAL APPROXIMATION METHOD ANALYSIS

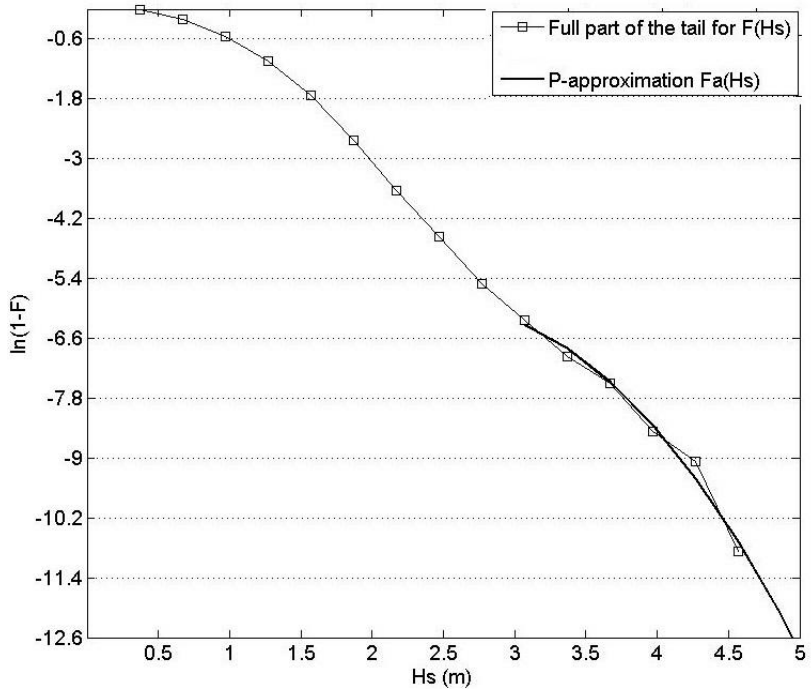

Fig. 5.51: Polynomial approximation method application for H_s at ERA IN-1 with parameters: N_T=6, n=2

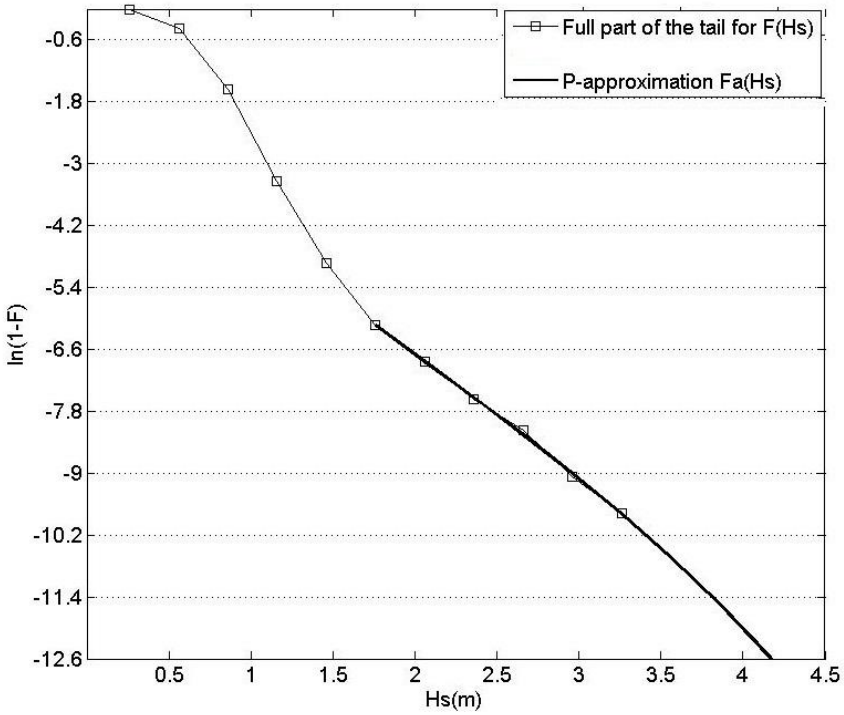

Fig. 5.52: Polynomial approximation method application for H_s at ERA IN-2 with parameters: N_T=6, n=3

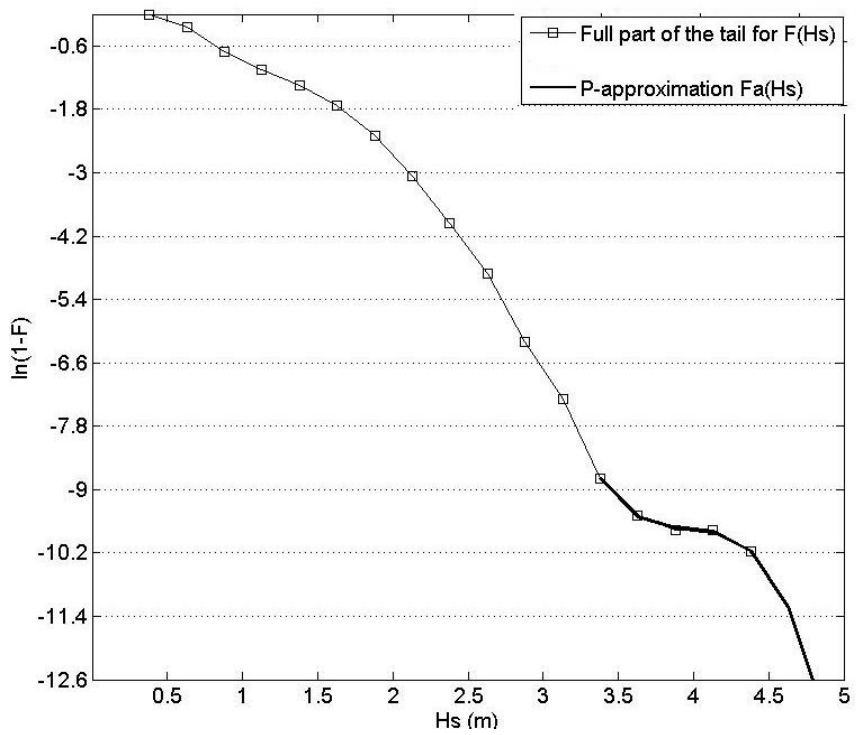

Fig. 5.53: Polynomial approximation method application for *Hs* at ERA IN-3 with parameters: N_T=5, n=3

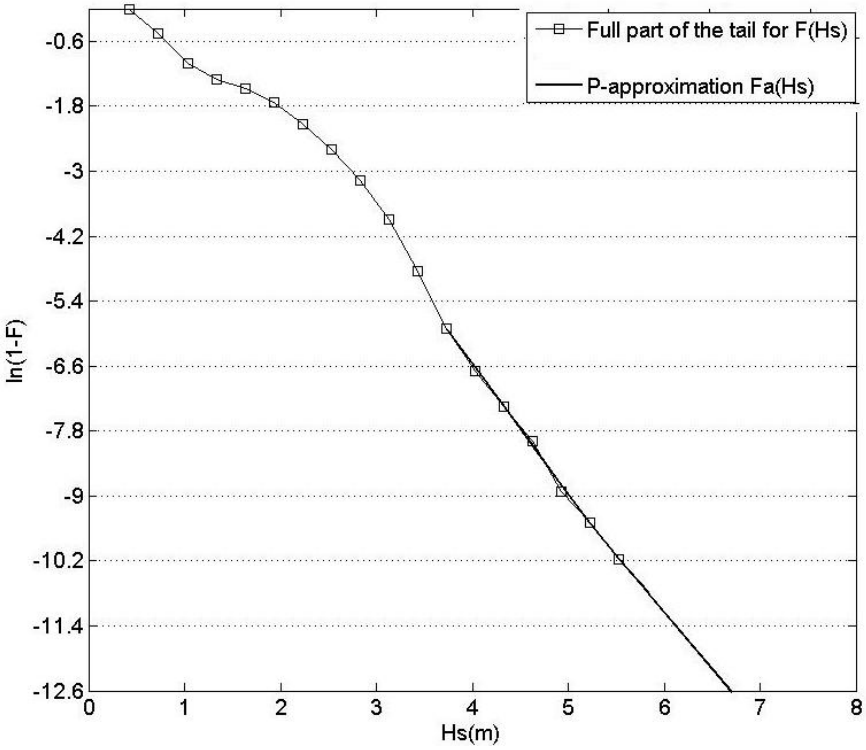

Fig. 5.54: Polynomial approximation method application for *Hs* at ERA IN-4 with parameters: N_T=7, n=2

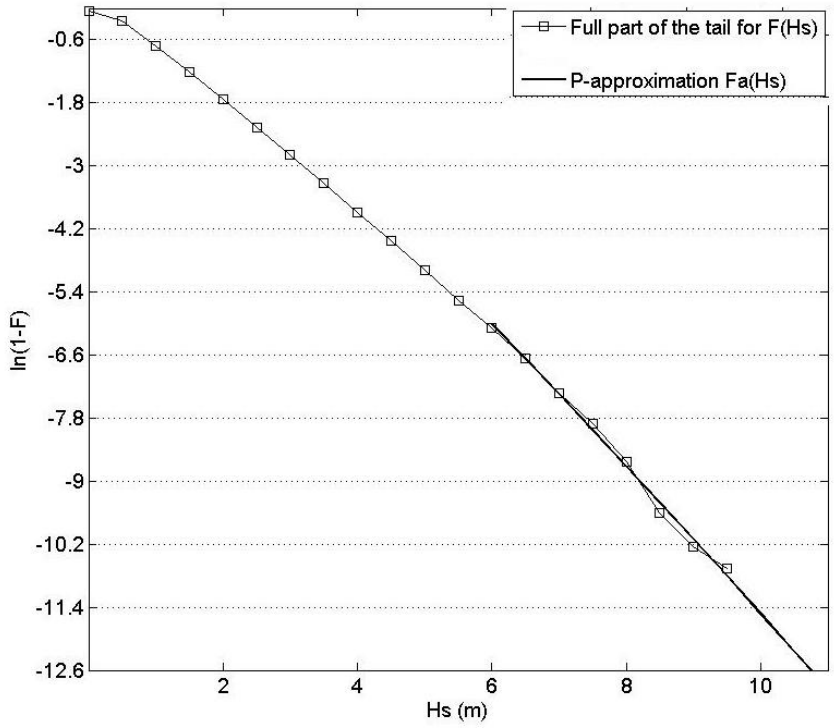

Fig. 5.55: Polynomial approximation method application for *Hs* at NOAA44005 with parameters: N_T=8, n=2

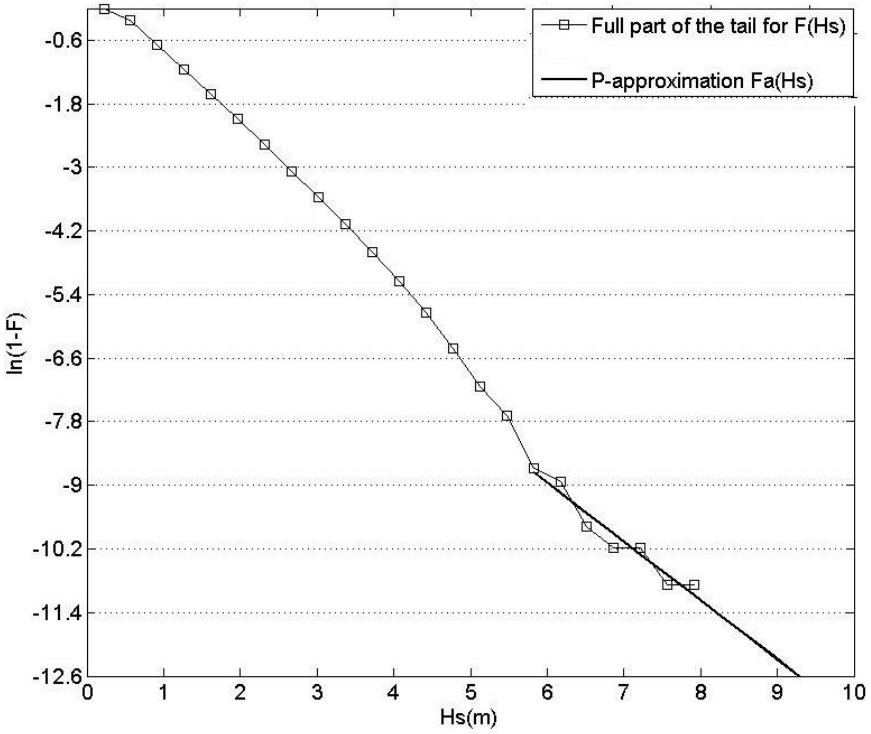

Fig. 5.56: Polynomial approximation method application for *Hs* at ERA44005 with parameters: N_T=7, n=1

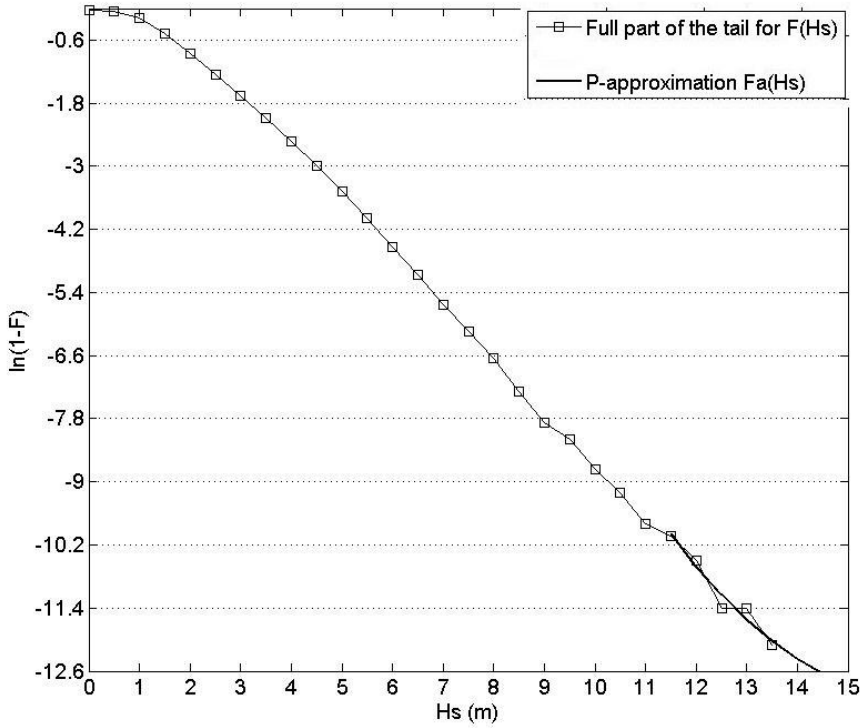

Fig. 5.57: Polynomial approximation method application for *Hs* at NOAA 46050 with parameters: N_T=5, n=2

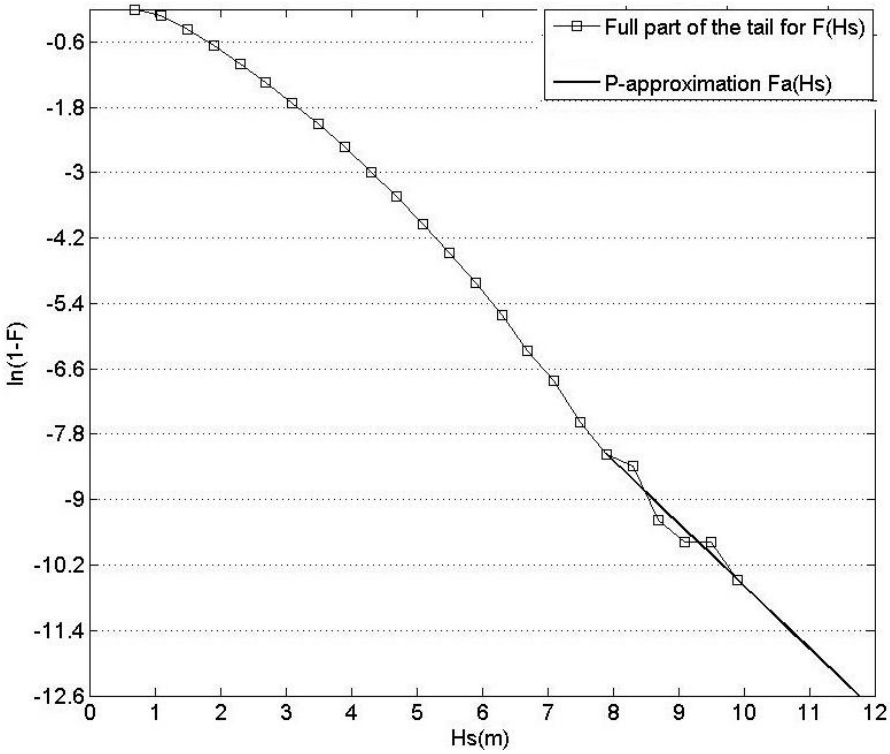

Fig. 5.58: Polynomial approximation method application for *Hs* at ERA 46050 with parameters: N_T=6, n=1

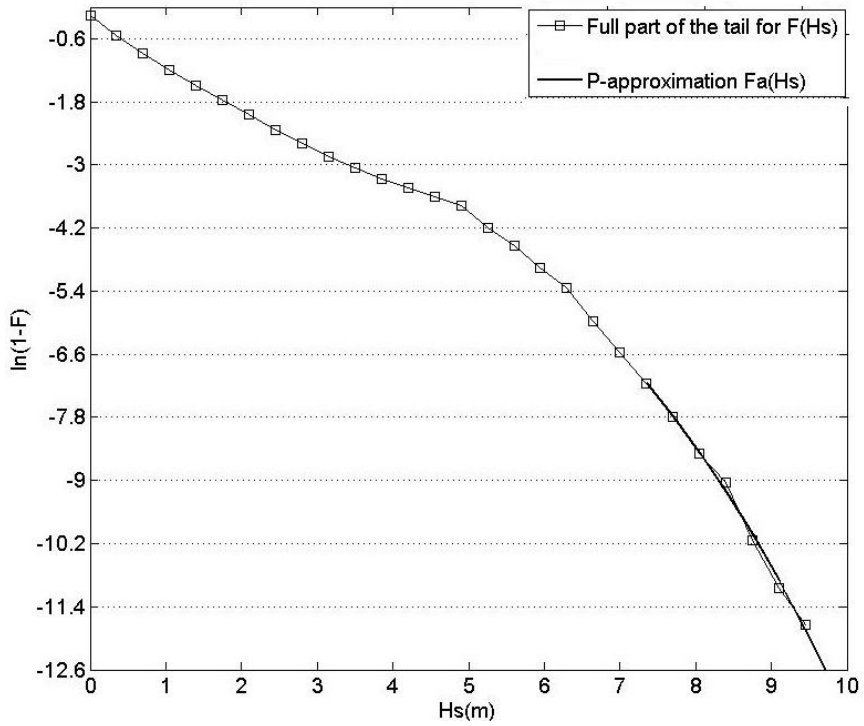

Fig. 5.59: Polynomial approximation method application for *Hs* at Alghero buoy with parameters: N_T=7, n=2

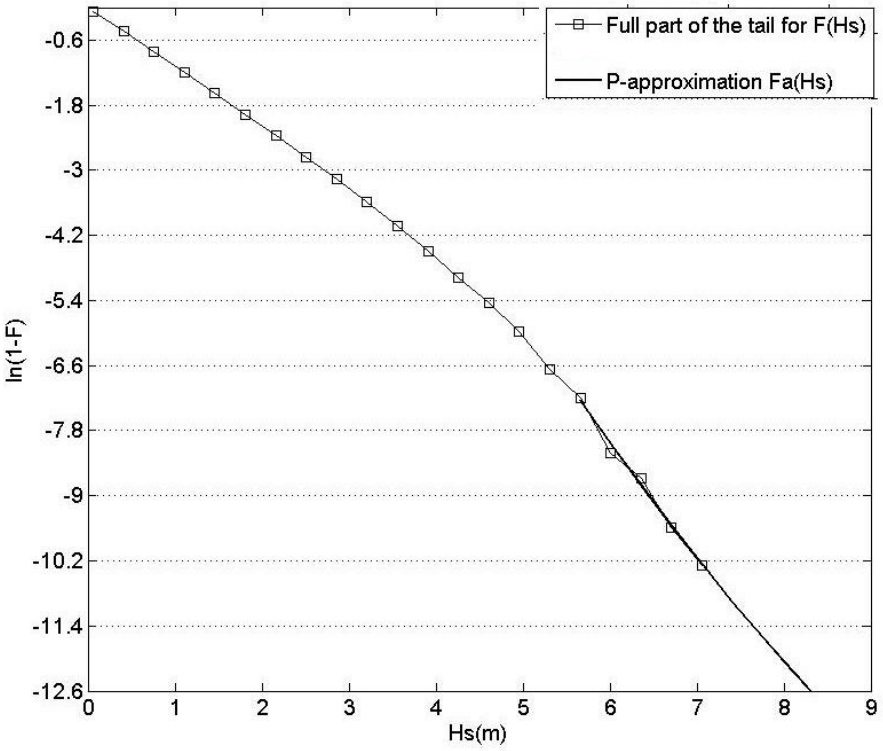

Fig. 5.60: Polynomial approximation method application for *Hs* at Alghero buoy with parameters: N_T=5, n=2

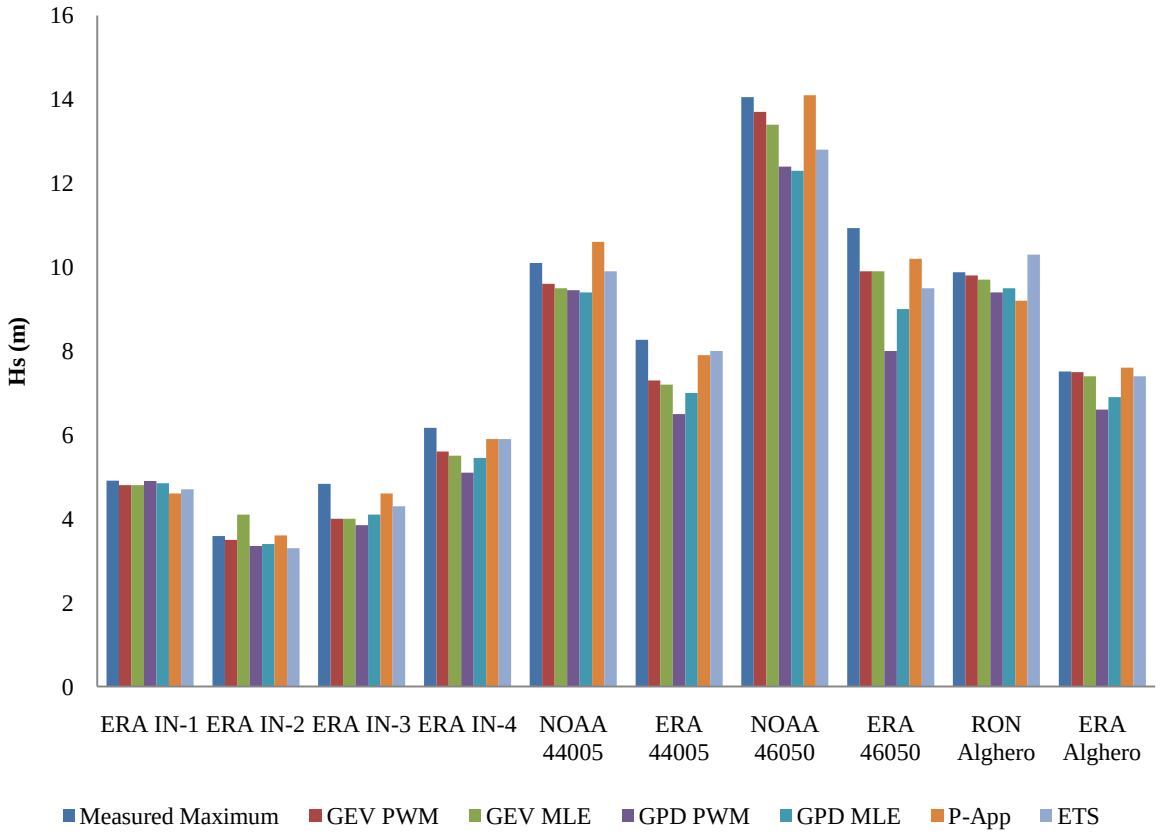

Fig. 3: Comparison of 30-yr values from different estimation models

Table 1: Percentage of variation of 30 year return value estimates from measured maximum wave height (%)

Data	GEV		GPD		P-App	ETS
	PWM	MLE	PWM	MLE		
ERA IN-1	-2	-2	0	-2	-6	-4
ERA IN-2	-3	14	-8	-5	0	-8
ERA IN-3	-17	-17	-19	-15	-5	-11
ERA IN-4	-9	-11	-17	-11	-4	-4
NOAA 44005	-5	-6	-6	-7	5	-2
ERA 44005	-12	-13	-21	-15	-4	-3
NOAA 46050	-2	-5	-12	-12	0	-9
ERA 46050	-9	-9	-27	-18	-7	-13
RON Alghero	-1	-2	-5	-4	-7	4
ERA Alghero	0	-1	-12	-8	1	-1

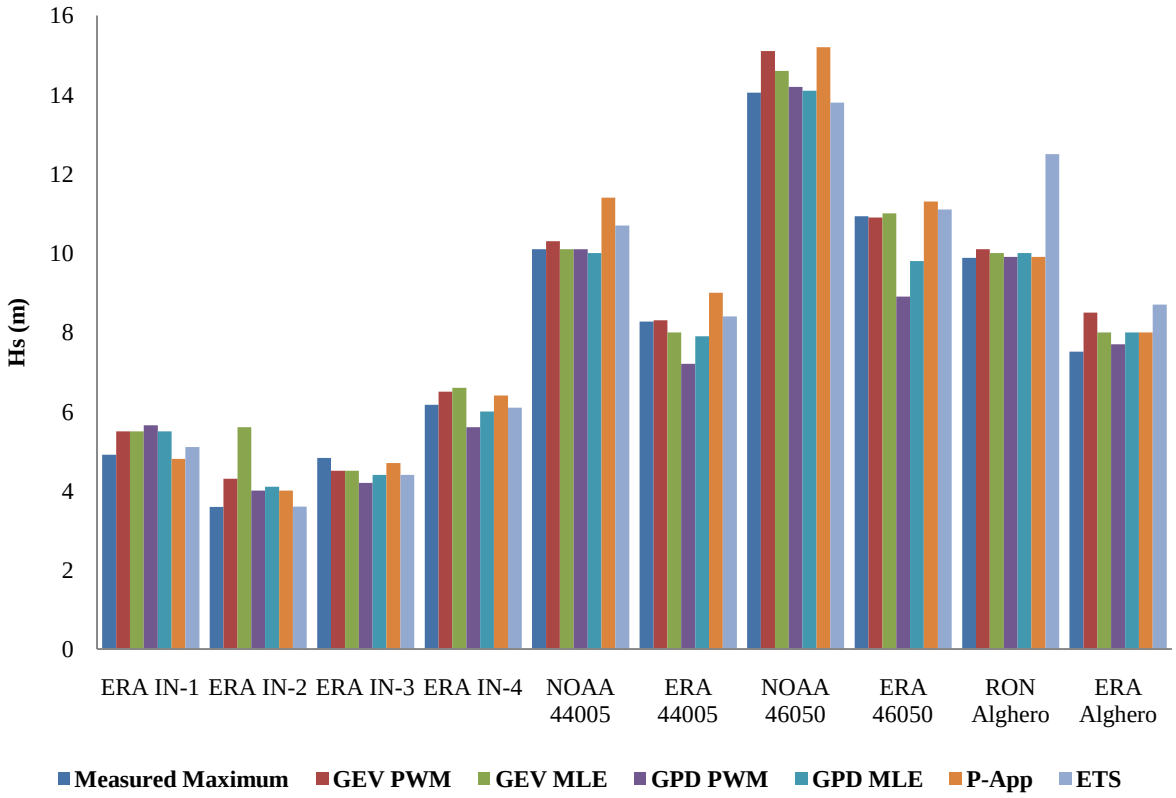

Fig. 4: Comparison of 100 year values from different estimation models

Table 2: Percentage of variation of 100 year return value estimates from measured maximum wave height (%)

Data	GEV		GPD		P-App	ETS
	PWM	MLE	PWM	MLE		
ERA IN-1	12	12	15	12	-2	4
ERA IN-2	20	56	11	14	11	0
ERA IN-3	-7	-7	-13	-9	-3	-9
ERA IN-4	5	7	-9	-3	4	-1
NOAA 44005	2	0	0	-1	13	6
ERA 44005	0	-3	-13	-4	9	2
NOAA 46050	7	4	1	0	8	-2
ERA 46050	0	1	-19	-10	3	2
RON Alghero	2	1	0	1	0	27
ERA Alghero	13	7	3	7	7	16